Holography of incoherently illuminated 3D scenes

Natan T. Shaked and Joseph Rosen

Department of Electrical and Computer Engineering, Ben-Gurion University
of the Negev, P.O. Box 653, Beer-Sheva 84105, Israel. natis@ee.bgu.ac.il

ABSTRACT

We review several methods of generating holograms of 3D realistic objects illuminated by incoherent white light. Using these methods, it is possible to obtain holograms with a simple digital camera, operating in regular light conditions. Thus, most disadvantages characterizing conventional holography, namely the need for a powerful, highly coherent laser and meticulous stability of the optical system are avoided. These holograms can be reconstructed optically by illuminating them with a coherent plane wave, or alternatively by using a digital reconstruction technique. In order to generate the proposed hologram, the 3D scene is captured from multiple points of view by a simple digital camera. Then, the acquired projections are digitally processed to yield the final hologram of the 3D scene. Based on this principle, we can generate Fourier, Fresnel, image or other types of holograms. To obtain certain advantages over the regular holograms, we also propose new digital holograms, such as modified Fresnel holograms and protected correlation holograms. Instead of shifting the camera mechanically to acquire a different projection of the 3D scene each time, it is possible to use a microlens array for acquiring the entire projections in a single camera shot. Alternatively, only the extreme projections can be acquired experimentally, while the middle projections are predicted digitally by using the view synthesis algorithm. The prospective goal of these methods is to facilitate the design of a simple, portable digital holographic camera which can be useful for a variety of practical applications.

Keywords: Digital and computer holography, Incoherent holography, Three-dimensional acquisition and processing.

1. INTRODUCTION

Holograms provide the most authentic three-dimensional (3D) illusion to the human eyes, with accurate depth cues, and without need for special viewing devices. Even if not reconstructed optically, holograms also have advantages as 3D models. By using holograms, 3D information can be stored in a very dense, efficient, and encrypted way. However, the conventional holographic recording process requires a coherent, powerful laser source and an extreme stability of the optical system as well as long developing process of the recorded hologram. The practical meaning of these disadvantages is that conventional holograms cannot be recorded outside a well-equipped optical laboratory.

Multiple viewpoint projection (MVP) holography is a method of generating digital holograms of 3D realistic objects illuminated by incoherent white light by using a digital camera. MVP holograms are generated by first acquiring multiple projections of a 3D scene from various perspective viewpoints, and then digitally processing the acquired projections to yield the digital hologram of the scene. In contrast to the composite hologram[1], an MVP hologram is equivalent to an optical hologram of the same scene recorded from the central point of view. The MVP acquisition is performed by a regular digital camera and under incoherent white light illumination, where neither an extreme stability of the optical system nor a powerful, highly coherent laser source is required.

The overall process of obtaining an MVP hologram can be divided into two main stages: the optical acquisition stage and the digital processing stage. In the acquisition stage, MVPs of the 3D scene are captured, whereas in the digital processing stage, mathematical operations are performed on these perspective projections in order to yield a complex function representing the digital hologram of the 3D scene. This complex function can be encoded into a computer generated hologram (CGH) with real and positive transparency values. Then, the recorded 3D scene can be reconstructed by illuminating the CGH transparency with a coherent plane wave[2]. As an alternative, the hologram can be reconstructed digitally by computing its Fresnel propagation along the optical axis, which reveals the recorded 3D scene slice by slice [2].

The current paper reviews different methods for capturing and processing MVP holograms, as well as presents selected experimental results. The capturing of the MVPs can be performed in several ways. For example, the digital camera can be shifted mechanically and acquire a different projection of the 3D scene from each perspective[2-5] (see subsection 2.1).

Instead of shifting the camera mechanically, it is also possible to utilize a microlens array (MLA) for acquiring the entire viewpoint projections in a single camera shot[6] (see subsection 2.2). Alternatively, a small number of extreme projections can be acquired by shifting the camera mechanically, while the middle projections are predicted digitally by using the view synthesis algorithm[7] (see subsection 2.3). It is also possible to use a hybrid of the two latter methods by utilizing a macrolens array to capture a small number of extreme high-resolution projections in a single camera shot and then predicting the middle projections while using the abovementioned view synthesis algorithm (see subsection 2.4).

Following the MVP capturing, the digital processing stage is carried out to yield the digital hologram of the 3D scene. Both one-dimensional (1D) MVP holograms[2,7-9] and two-dimensional (2D) MVP holograms[3-6,9] can be produced, depending on the camera movement (see subsection 3.1). The digital process itself includes multiplication of each projection by a certain complex function and the sum of the inner product is introduced into the corresponding pixel of the 2D hologram matrix. In case of the 1D hologram, the sum of the 1D inner product is the corresponding column in the hologram matrix. After choosing the hologram dimensionality (1D or 2D), several types of MVP holograms can be generated depending on the nature of the digital process applied to the acquired projections, or more specifically, by the nature of the certain complex function used to multiply the projections. Several types of MVP holograms have been reported in the literature. These include Fourier holograms[2-5] (see subsection 3.2) and Fresnel holograms[4,5] (see subsection 3.3), as well as new types of digital holograms proposed due to their certain advantages over the known types of holograms. The digital incoherent modified Fresnel hologram (DIMFH)[8,9] (see subsection 3.4) is an example of these new types of holograms. By using the DIMFH, a Fresnel hologram can be obtained straightforwardly, without redundant calculations, approximations, or assumptions. Another type of new hologram is the digital incoherent protected correlation hologram (DIPCH)[9] (see subsection 3.5). Using this hologram, it is possible to transfer encrypted 3D information in a secured way. In addition, this hologram, compared to the DIMFH, has a significantly improved reconstruction resolution for far objects in the 3D scene.

2. CAPTURING THE MULTIPLE PROJECTIONS

As mentioned above, in order to capture the MVPs, it is possible to use several methods which include shifting the camera mechanically, spatial multiplexing, or digital synthesis of the middle projections. This section reviews each of these methods and presents experimental results for some of them.

2.1 Shifting the camera

In Refs. [2-5], the projections were acquired by shifting the camera mechanically, so that in each location the camera captured only a single perspective projection. This is the first method our group has implemented, since it does not require any additional hardware or capturing algorithms. However, this acquisition process is quite slow, especially if a 2D hologram is acquired. For example, a 2D MVP hologram with 256×256 pixels requires 65536 projections. This is a large number of projections and it is quite hard to capture these projections by using manual shifts of a micrometer. A step motor has been used to make this process faster and more accurate. However, the mechanical movement of the camera, even if performed by using a step motor, is not adequate when the object moves faster than one cycle of acquisition, since wrong perspective projections will be captured in that situation. Therefore, there is a need for the alternative capturing methods described next.

2.2 Spatial multiplexing

In order to avoid the mechanical movements of the camera, a spatial-multiplexing MVP acquisition can be used. Positioning several cameras in an array is one option to do this. However, the method requires multiple cameras, and as a result the entire camera array is quite expensive. Instead, in Ref. [6], we proposed to use an MLA to capture simultaneously a large number of projections in a single camera shot. This acquisition method is similar to that usually used in the integral imaging field[10]. However, here the goal is to produce an incoherent hologram which can be reconstructed optically, without the need for the MLA. Figure 1(a) shows the optical system used for capturing the multiple projections by using the MLA. A plano-convex lens L_1, positioned at a distance of its focal length f_1 from the 3D scene, is attached to the MLA and utilized to collimate the beams coming from the 3D scene and thus to increase the number of microlenses participating in the process. A spherical lens L_2, with a focal length of f_2, projects the MLA image plane upon the camera with the magnification of $-z_2/z_1$. Then, the camera captures the entire MLA image plane in a single shot and sends the image to the computer for the processing stage. Figures 1(b) show several chosen projections cut from different parts of the overall MLA image plane captured by the camera. As seen in these figures, the relative
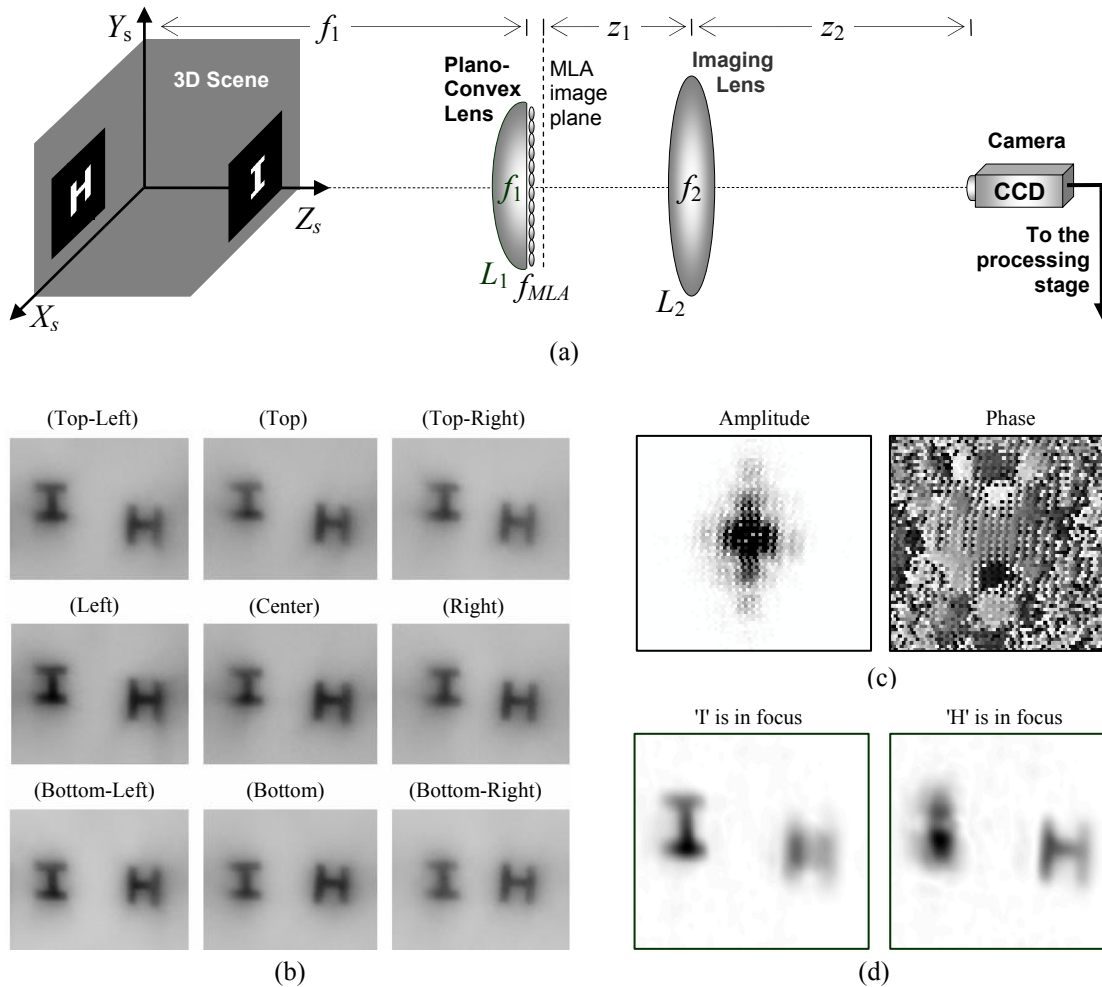
Fig. 1. (a) Optical system for capturing the multiple projections by using an MLA; (b) Several projections taken from different parts of the MLA image plane captured by the camera; (c) Magnitude and phase of the Fourier hologram obtained after performing the processing stage on the captured projections; (d) Reconstruction of the hologram at the best-focus distances. Note: the pictures appearing in (b)-(d) are contrast-inverted for better visualization.

positions of the two letters change as a function of the location of the projection on the entire MLA image plane. This is the effect that leads to the 3D properties of the hologram obtained in the end of the digital process. After the acquisition of the MVPs, different types of MVP holograms can be obtained depending on the digital process carried out on the acquired projections. These possible digital processes are discussed in Section 3. Figures 1(c) show the Fourier hologram (the digital process of which is described in subsection 3.2) that has been produced by using the acquired projections. Reconstructing this hologram can be done optically, by illuminating its inverse Fourier transform with a coherent plane wave or instead, digitally by first inverse Fourier transforming it, and then simulating a Fresnel propagation along the optical axis. The purpose of this propagation is to reveal different planes along the optical axis of the 3D reconstruction. The two best in-focus reconstructed planes are shown in Figs. 1(d). The fact that in each reconstructed plane only a single letter, the 'I' or the 'H', is in focus whereas the other letter, the 'H' or the 'I' respectively, is out of focus validates that a volume information is indeed encoded into the hologram.

However, since each projection yields only a single pixel in the hologram, the resolution of the hologram shown in Figs. 1(c) is quite low (only 65×65 microlenses are used in this case, where each microlens yields a single projection and hence a single pixel in the hologram). To obtain a high resolution hologram, an array containing many microlenses is

needed. Still, since the total size of the microlens array is limited, having more microlenses in the array means that the diameter of each single microlens is quite small. This results in a low resolving power of each microlens, causing a poor imaging resolution in each projection. On the other hand, having a microlens with a bigger diameter leads to a better imaging resolution of each projection, but then fewer microlenses can be used, and hence there are fewer pixels in the hologram. To solve this problem, the next subsections present alternative MVP acquisition methods.

2.3 Shifting the camera for the extreme projections and synthesizing the middle projections digitally

In Ref. [7], we have presented a way to reduce the number of perspective projections, so that the camera acquires only a small number of projections, typically the extreme ones. Then the computer synthesizes the middle projections by using a 3D interpolation algorithm called the view synthesis algorithm[11]. Given two viewpoint projections, the algorithm first calculates the correspondence map, containing the displacements of each pair of corresponding pixels in the two given projections, and then predicts how the scene would look from new viewpoints by interpolating the locations and intensities of the corresponding pixels in the two given projections. In Ref. [7], the camera moves mechanically to acquire the MVPs. Therefore, in spite of reducing the number of perspective projections and still capturing projections in an acceptable resolution, there is still a problem in utilizing this acquisition method to generate holograms of moving bodies.

## 2.4 Using a macrolens array and synthesizing the middle projections digitally

To obtain MVP holograms of moving bodies and still to get an acceptable resolution of each projection, we hybridize both methods presented in subsections 2.2 and 2.3 above. This is performed by building two new macrolens arrays. The first array, shown on the left side of Fig. 2(a), contains 3×3 negative lenses. To produce this array, we used nine standard negative lenses, each of which had a focal length of −25 cm and an original diameter of 5 cm. To take advantage of the entire array size, each lens was cut into a square of 3.53×3.53 cm, and a 3×3 macrolens array of 10.6×10.6 cm was formed by sticking together the cut lenses with an optical adhesive (Norland 61) under a UV source. The second array, shown on the right side of Fig. 2(a), was built in a similar way. This array contains 5×5 negatives lenses, each with the focal length of −12.5cm and an original diameter of 2.5 cm. The lenses were cut into squares of 1.76×1.76 cm each, so that the final 5×5 macrolens array, obtained after sticking all the lenses together, was 8.8×8.8 cm in size. Figure 2(b) shows the 3×3 projections acquired by the first array, whereas Fig. 2(c) shows the 5×5 projections acquired by the second array. These macrolens arrays provide a convenient way to capture a small number of projections on a 2D grid simultaneously. Thus, it is possible to acquire the projections of a moving body. After the projections are acquired, the view synthesis algorithm is applied, so that the middle projections are synthesized. Then, a digital hologram of the observed 3D scene can be created by applying one of the digital processes, described in the next section, to the entire set of perspective projections.

## 3. PROCESSING THE CAPTURED PROJECTIONS INTO A HOLOGRAM

The digital process, carried out on the acquired MVPs actually determines the type of hologram which is generated. Our group has shown[2,3,5-9] that by processing the MVPs it is possible to generate Fourier, Fresnel, image, modified Fresnel and protected correlation holograms. In addition, for each of the above types, it is possible to generate both 1D and 2D MVP holograms. This section reviews the digital processes that should be applied for each of these holograms.

3.1 One-dimensional and two-dimensional MVP holograms

The nature of the camera movement determines the hologram dimensionality (1D or 2D). The 1D holograms[2,7-9] are easier to produce because the projections needed for this kind of holograms are captured along a single transverse axis only, unlike the 2D holograms in which the projections are captured on a transverse 2D grid. However, 2D holograms have the advantage of encoding the 3D information into both axes. This advantage can be demonstrated by the following example. Let us assume we record a 1D hologram of an object with the shape of a thin long horizontal line, where the camera moves along the long dimension of this line-shaped object. The axial location of the object is actually lost in the hologram processing, and the reconstructed image is in-focus along a long range on the optical axis. On the other hand, the 2D holograms contain the axial information, no matter what the shape of the recorded object is, and the image of the line-shaped object in the example above is in focus only in a single well-defined transverse plane, as it is supposed to be.
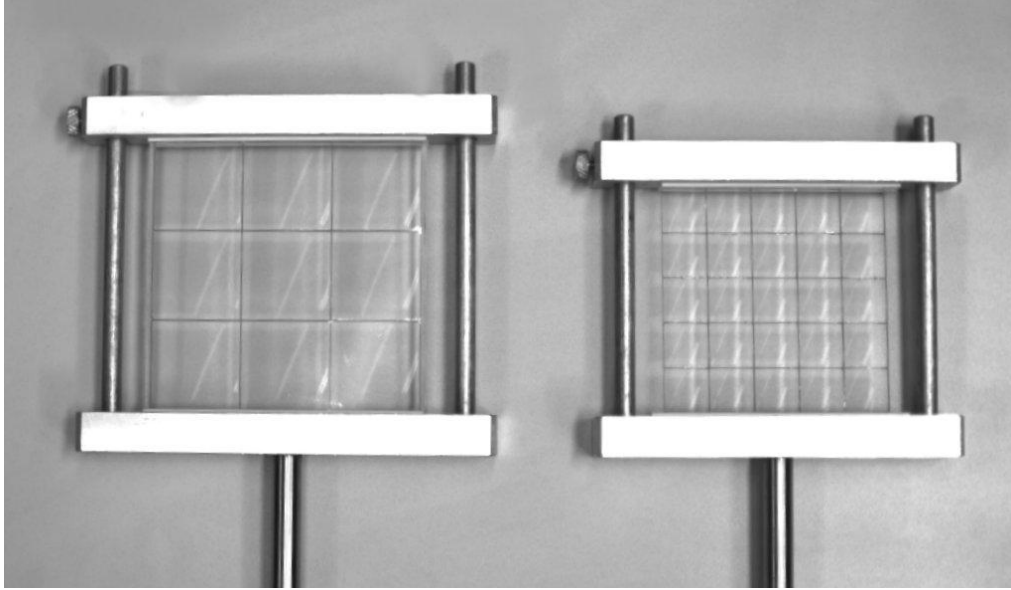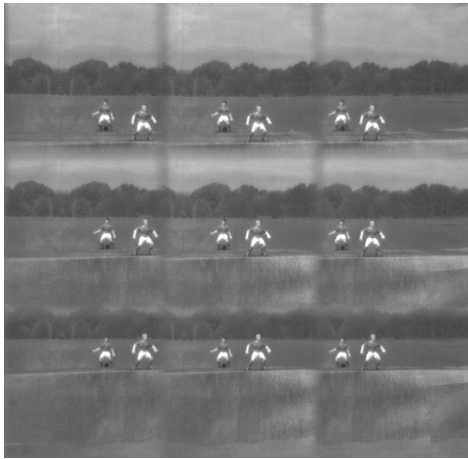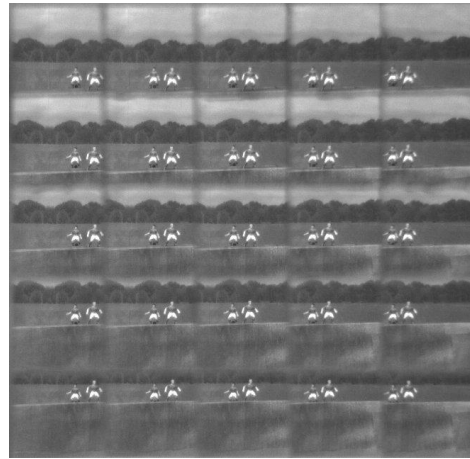
Fig. 2. (a) 3×3 macrolens array (left) and 5×5 macrolens array (right); (b) The image plane of the 3×3 macrolens array; (c) The image plane of the 5×5 macrolens array.

In the case of a 1D MVP hologram, let us assume that $2K+1$ projections of the 3D scene are acquired along the horizontal axis only. We number the projections by m, so that the middle projection is denoted by $m = 0$, the right projection by $m = K$ and the left projection by $m = -K$. Then, to generate a 1D MVP hologram, each row of the m-th projection $P_m(x_p, y_p)$ is multiplied by a certain point spread function (PSF) and the products are summed up into the (m,n)-th pixel in a complex matrix as follows:

$$H_1(m,n) = \iint P_m(x_p, y_p) E_1(x_p, y_p - n\Delta p) dx_p dy_p, \qquad (1)$$

where $E_1(x_p, y_p)$ represents the generating PSF of the 1D hologram, x_p and y_p are the axes on the projection plane, n is the row number in the complex matrix H_1, and Δp is the pixel size of the digital camera. $E_1(x_p, y_p)$ is defined as the following:

$$E_1(x_p, y_p) = A_1(b_x x_p) \exp\left[ig_1(b_x x_p)\right]\delta(y_p),$$ (2)

where A_1 and g_1 are general functions dependent on x_p only, and may be defined differently for every type of MVP hologram, b_x is an adjustable parameter (with units that preserve the arguments of A_1 and g_1 as unitless quantities) which may or may not be dependent on the projection index m, and δ is the Dirac delta function. According to Eq. (1), each projection contributes a different column to the complex matrix $H_1(m, n)$ which represents, in the end of the digital process, the 1D MVP hologram of the 3D scene.

Excluding Fourier holograms, to obtain the reconstructed planar image $s_1(m, n; z_r)$ located at an axial distance z_r from the 1D hologram, the hologram is digitally convolved with a reconstructing PSF as follows:

$$s_1(m, n; z_r) = \left| H_1(m, n) * R_1(m; z_r) \right|,$$ (3)

where * denotes a 1D convolution, and $R_1(m; z_r)$ is the reconstructing PSF of the 1D hologram. This PSF is given by:

$$R_1(m; z_r) = A_1\left(\frac{m\Delta p}{z_r}\right) \exp\left[-ig_1\left(\frac{m\Delta p}{z_r}\right)\right],$$ (4)

where A_1 and g_1 are the same functions used for the generating PSF of the 1D hologram [Eq. (2)].

In the case of a 2D MVP hologram, let us assume that horizontal (2K+1) by vertical (2K+1) MVPs are acquired. We number the projections by m and n, so that the middle projection is denoted by $(m,n) = (0,0)$, the upper-right projection by $(m,n) = (K,K)$, and the lower-left projection by $(m,n) = (-K,-K)$. Then, to generate a 2D MVP hologram, the (m,n)-th projection $P_{m,n}(x_p, y_p)$ is multiplied by a certain PSF and the product is summed up into the (m,n)-th pixel in a complex matrix as follows:

$$H_2(m, n) = \iint P_{m,n}(x_p, y_p) E_2(x_p, y_p) dx_p dy_p,$$ (5)

where $E_2(x_p, y_p)$ represents the generating PSF of the 2D hologram. This PSF is defined as the following:

$$E_2(x_p, y_p) = A_2(b_x x_p, b_y y_p) \exp\left[ig_2(b_x x_p, b_y y_p)\right],$$ (6)

where A_2 and g_2 are general functions dependent on (x_p, y_p) and may be defined differently for every type of MVP hologram as discussed below. b_x and b_y are adjustable parameters (with units that preserve the arguments of A_2 and g_2 as unitless quantities) which may or may not be dependent on m and n, respectively. The process manifested by Eq. (5) is repeated for all of the projections, but in contrast to the 1D case, in the 2D case each projection contributes a single pixel to the hologram matrix rather than a column of pixels. In the end of this digital process, the obtained 2D complex matrix $H_2(m, n)$ represents the 2D MVP hologram of the 3D scene.

Excluding Fourier holograms, the reconstructed planar image $s_2(m, n; z_r)$ located at an axial distance z_r from the 2D hologram is obtained by digitally convolving the hologram with a reconstructing PSF as follows:

$$s_2(m, n; z_r) = \left| H_2(m, n) * R_2(m, n; z_r) \right|,$$ (7)

where, this time, * denotes a 2D convolution, and $R_2(m, n; z_r)$ is the reconstructing PSF of the 2D hologram. This PSF is given by:

$$R_2(m, n; z_r) = A_2\left(\frac{m\Delta p}{z_r}, \frac{n\Delta p}{z_r}\right) \exp\left[-ig_2\left(\frac{m\Delta p}{z_r}, \frac{n\Delta p}{z_r}\right)\right],$$ (8)

where A_2 and g_2 are the same functions used in the generating PSF of the 2D hologram [Eq. (6)]. The above reconstructing PSFs, given by Eqs. (4) and (8), are applied for a digital reconstruction. Optical reconstruction of Fourier and Fresnel holograms can be performed by illuminating them with a coherent plane wave, whereas in the Fourier hologram case, the hologram has to be inverse Fourier transformed first (by a Fourier lens, for example). Therefore, even if a new type of digital hologram is defined so that this hologram can only be reconstructed digitally by using the PSF of Eq. (4) or (8), an optical reconstruction of this hologram can still be obtained by digitally converting this hologram to a

regular type of hologram (such as Fourier or Fresnel). Another possibility is to reconstruct this special hologram optically by using an optical correlator[12].

In order to simulate an optical reconstruction, Fresnel propagation can be implemented digitally by using Eq. (7), where in this case $R_2(m,n;z_r)$ is a 2D quadratic phase function given by:

$$R_2(m,n;z_r) = \exp\left[-i\frac{(m\Delta p)^2 + (n\Delta p)^2}{z_r}\right]. \tag{9}$$

3.2 Fourier holograms

To employ the MVPs for generating a 1D Fourier hologram, Eq. (1) should be used, where the PSF of the 1D Fourier hologram is as follows:

$$E_1(x_p, y_p) = \exp(ibmx_p)\delta(y_p), \tag{10}$$

where b is an adjustable parameter. Similarly, in order to use the MVPs to generate a 2D Fourier hologram, Eq. (5) should be used, where the PSF of the 2D Fourier hologram is given by:

$$E_2(x_p, y_p) = \exp(ibmx_p + ibny_p). \tag{11}$$

This means that the generation of MVP Fourier holograms is performed by multiplying each of the MVPs by a different linear phase function with a frequency that is dependent on the relative position of the projection in the entire projection set. This type of hologram was generated in Refs. [2-7]. In the mathematical proof of the method[2], it is shown that the method is valid only if we assume that the MVPs are acquired across a relatively narrow angular range (30-40 degrees). An example of a Fourier MVP hologram is shown in Figs. 1(c).

3.3 Fresnel and image holograms

According to Refs. [4] and [5], it is possible to generate Fresnel, image, and other types of holograms by using an MVP Fourier hologram generated beforehand. The basic idea is to take the Fourier hologram obtained by the method elaborated in subsection 3.2 and to inverse Fourier transform it. Then, by a digital Fresnel propagation (convolution with quadratic phase functions), either Fresnel hologram or image hologram can be obtained, depending on the propagation distance.

However, there are several disadvantages of this method. First, since the generation of the Fresnel, or other types of Fourier-based holograms is performed indirectly, the resulting hologram is approximated and inaccurate, as well as requires redundant calculations. Digital errors may also occur during the various transformations. Moreover, since the original Fourier hologram is limited to small angles, the resulting holograms are limited to small angles as well.

3.4 Modified Fresnel hologram (DIMFH)

The DIMFH[8,9] is generated by processing the MVPs directly rather than performing a Fresnel propagation on the reconstructed Fourier hologram as presented in subsection 3.3. Hence, redundant calculations and digital errors during the various transformations are avoided. Furthermore, this direct Fresnel holography method is not limited to small angles, and therefore the hologram reconstruction is more accurate. Since the prospective goal of these white light holography methods is to facilitate the design of a portable digital holographic camera, it is important to use digital calculations as few as possible. Avoiding redundant calculations becomes extremely critical when Fresnel holograms with a large number of pixels have to be calculated.

The 1D DIMFH is generated by multiplying each projection by the following 1D quadratic phase function:

$$E_1(x_p, y_p) = \exp(i2\pi b^2 x_p^2)\delta(y_p), \tag{12}$$

and summing up the product, according to Eq. (1), into a column in the final hologram matrix. Similarly, the 2D DIMFH processing is carried out by multiplying each projection by the following 2D quadratic phase function:

$$E_2(x_p, y_p) = \exp\left[i2\pi b^2(x_p^2 + y_p^2)\right], \tag{13}$$

and summing up the product, according to Eq. (5), into the corresponding pixel in the final 2D hologram. Note that opposite to the digital process of the MVP Fourier hologram, in the DIMFH (as well as in the DIPCH presented next) the PSF is independent from the projection indices m and n. Since each projection is multiplied by the same spatial function, this process is a spatial correlation between the observed 3D scene and the PSF and therefore, the resulting matrix is termed incoherent correlation hologram. However, in contrast to other correlation holograms[12,13], the present holograms are created from real existing objects illuminated by incoherent white light.

It has been shown in Refs. [8] and [9] that the transverse and the longitudinal magnifications of 1D incoherent correlation holograms are given by:

$$M_{1,x} = \frac{\Delta p}{\alpha}; \quad M_{1,y} = \frac{f}{z_s} = M; \quad M_{1,z} = \frac{\Delta p}{bf\alpha}, \tag{14}$$

where α is the gap between two adjacent projections, f is the focal length of the imaging lens, z_s is the axial coordinate of the inspected object, and M is the magnification of the imaging lens. Similarly, the magnifications of 2D incoherent correlation holograms are given by:

$$M_{2,x} = M_{2,y} = \frac{\Delta p}{\alpha}; \qquad M_{2,z} = \frac{\Delta p}{bf\alpha}. \tag{15}$$

It is evident from Eqs. (14) and (15) that contrary to the conventional holograms, the magnifications of correlation holograms on the acquisition axes (x for the 1D case and x-y for the 2D case) are independent from the axial positions of the objects in the 3D scene. This behavior is explained intuitively next. Although farther objects look smaller than closer objects in each captured projection, they also 'move' slower throughout the projections because of the parallax effect. The slower 'movement' broadens the correlation with the PSF in a way that the reduction of the image size in each projection is precisely compensated by the increment of the correlation size. This feature can be very useful for pattern recognition for example, as we intend to show in our future work. However, this effect can also be eliminated during the reconstruction process. To do this, the reconstructed image should be scaled by $M/M_{1,x} = (f/z_s)/(\Delta p/\alpha) = 1/(bz_r)$ [since $z_r/z_s = \Delta p/(bf\alpha)$] across the acquisition axes for each and every reconstructed plane. This scaling process is demonstrated next for the 1D case.

To generate and reconstruct incoherent correlation holograms, we implemented, in Ref. [9], the optical system illustrated in Fig. 3(a). Three equal-size USAF resolution charts, 8.5×8.5 cm each, were printed and positioned at the scene in front of a dark background and were illuminated by a Halogen white light. The digital camera was positioned on a micrometer slider and captured 1200 projections of the 3D scene across a horizontal range of 24 cm. Since the goal was just to check the feasibility of the digital process of incoherent correlation holograms, we chose the more-primitive MVP acquisition method in which the camera was shifted mechanically and captured a single projection each time. Figs. 3(b) show the two most-extreme and central projections out of the 1200 projections captured by the camera. Based on these projections, we generated a 1D DIMFH, according to Eqs. (1) and (12), by multiplying each projection by the 1D quadratic phase function, and summing up the result into the corresponding column in the 1D DIMFH. The amplitude and phase of the resulting 1D DIMFH are shown in Figs. 4. According to Eqs. (3) and (4), the reconstruction of this 1D DIMFH was carried out by 1D convolution of the hologram with 1D quadratic phase functions having a phase sign opposite to that of the generating PSF. The three best in-focus reconstructing PSFs and the corresponding best in-focus reconstructed planes are shown in Figs. 5(a) and 5(b), respectively. In each of the planes shown in Figs. 5(b), a different USAF resolution chart is in focus, whereas the other two charts are out of focus. This validates the success of the holographic process of the 1D DIMFH. As explained above, resampling these reconstructed planes along the horizontal axis is required for retaining the original aspect ratios of the objects. These resampled best in-focus reconstructed planes are shown in Figs. 5(c). Figures 5(d) show the corresponding zoomed-in images of the best in-focus charts. From this figure, one can conclude that the far objects in the 3D scene have a reduced horizontal reconstruction resolution compared to the close objects in the scene. In the next subsection, we show that there is also a difference in the resolution reduction between the DIPCH and the DIMFH for the far objects in the scene.

(a)

| Left | Middle | Right |
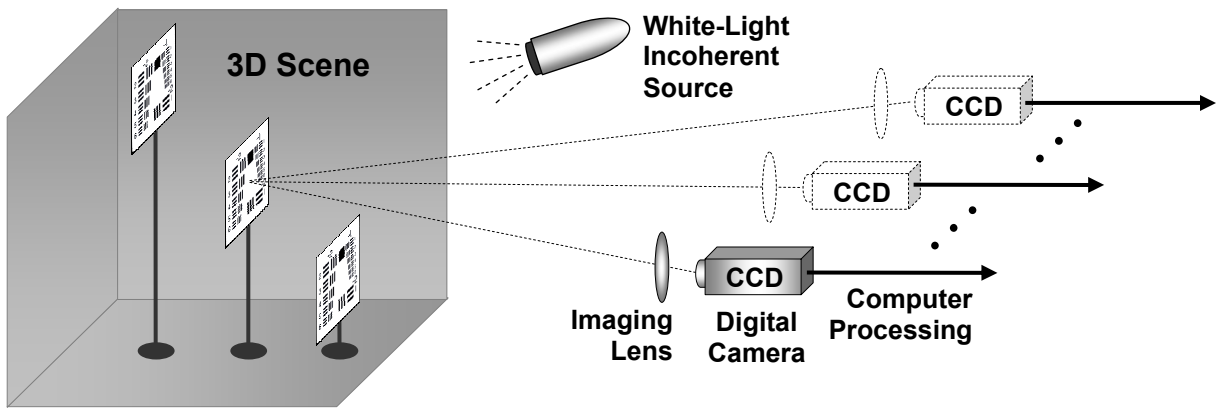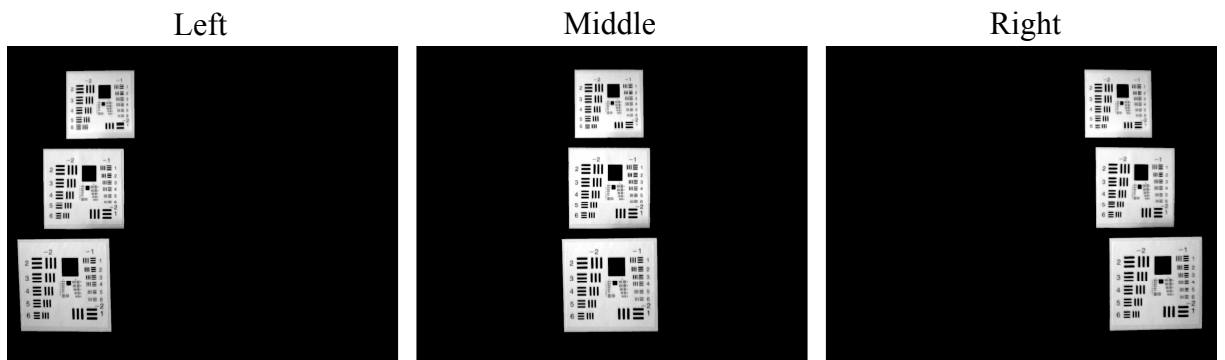
(b)

Fig. 3. (a) The optical system for acquiring MVPs of the 3D scene along the horizontal axis;
(b) Several projections taken from the entire experimentally-obtained set containing 1200 projections.
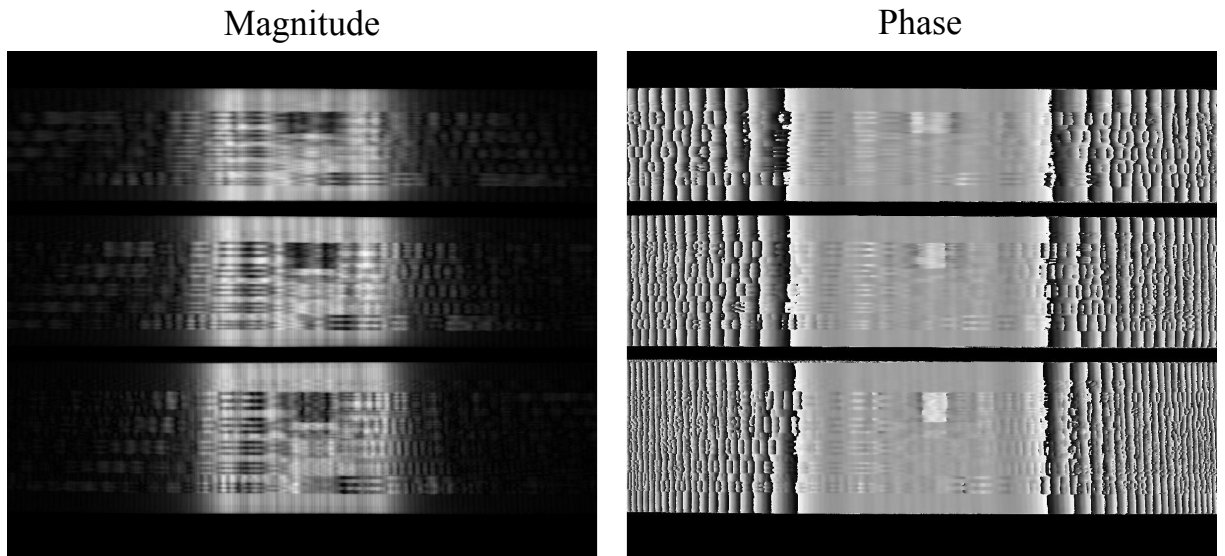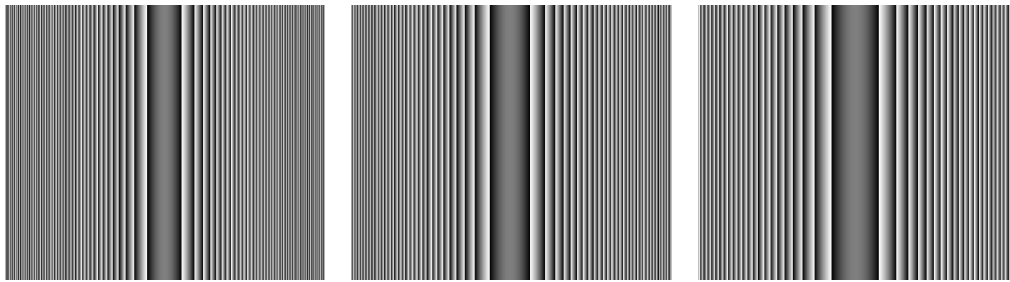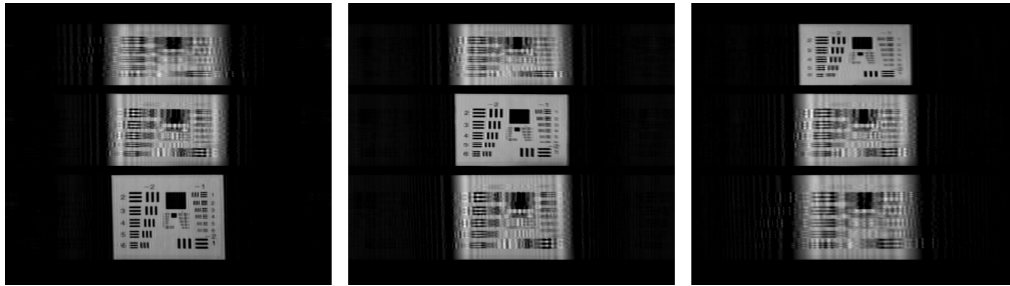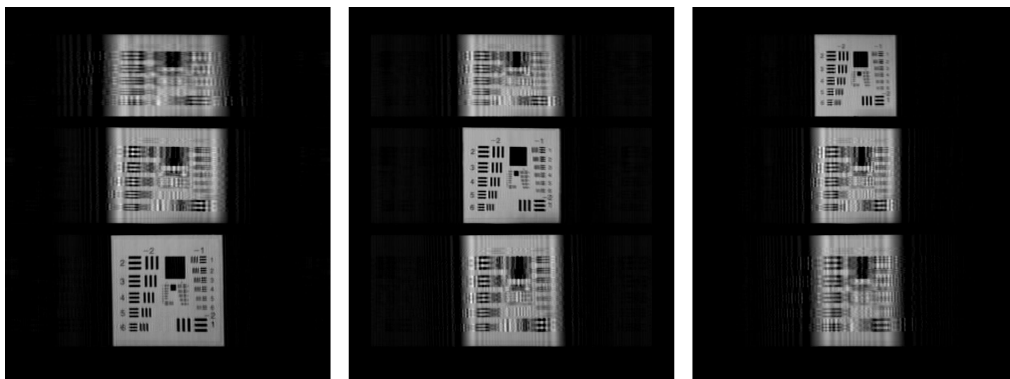
Magnitude   Phase

Fig. 4. Magnitude and phase of the 1D DIMFH obtained from the MVP set, partially shown in Figs. 3(b).
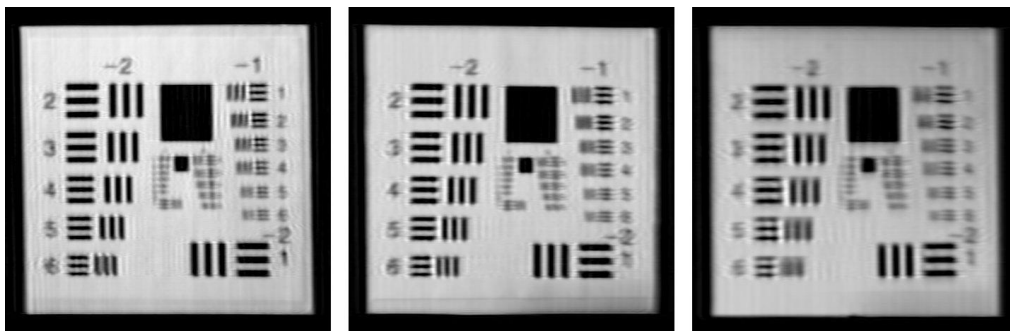
Fig. 5. Reconstructing the 1D DIMFH shown in Figs. 4: (a) The phase distributions of the reconstructing PSFs used for obtaining the three best in-focus reconstructed planes; (b) The corresponding three best in-focus reconstructed planes along the optical axis; (c) Same as Figs. 5(b), but after the resampling along the horizontal axis; (d) Zoomed-in images of the corresponding best in-focus reconstructed objects.

3.5 Protected correlation hologram (DIPCH)

The DIPCH[9] is another type of incoherent correlation hologram. This hologram has two advantages over the Fresnel hologram in general, and over the DIMFH in particular. First, since a random-constrained PSF is used to generate the hologram, only an authorized user who knows this PSF can reconstruct the scene encoded into the hologram. Thus, the DIPCH can be used as a method of encrypting the observed scene. Second, the reconstruction obtained from the DIPCH, compared to the DIMFH, has a significantly higher transverse resolution for the far objects in the 3D scene.

The 1D DIPCH process is still defined by Eqs. (1) and (3). However, this time, the generating PSF is a space-limited random function which fulfills the constraint that its Fourier transform is a phase-only function. In order to find this PSF, we used the projection onto the constraint sets (POCS) algorithm[14,15]. The POCS algorithm, used to find this PSF, is illustrated in Fig. 6(a). The POCS is an iterative algorithm which bounces from the PSF domain to its spatial spectrum domain and back, using Fourier transform (FT) and inverse Fourier transform (IFT). In each domain, the function is projected onto the constraint set. The two constraints of the POCS express the two properties required for the PSF of the DIPCH. First, the FT of the PSF should be a phase-only function. This requirement enables to reconstruct the DIPCH properly. So, the constraint of the POCS in the spectral domain is the set of all phase-only functions, and each Fourier transformed PSF is projected onto this constraint by setting its magnitude distribution to the constant 1. The other property of the PSF is that it should be space limited into relatively narrow region close to, but outside the origin. This condition reduces the reconstruction noise from the out-of-focus objects because the overlap, occurring during the cross-correlation between the resampled space-limited reconstructing PSF and the hologram in out-of-focus regions, is lower than the overlap in case of using a wide-spread PSF. Of course, the narrower the existence region of the PSF, the lower the noise is. However narrowing the existence region makes it difficult for the POCS algorithm to converge to a PSF that satisfies both constraints within an acceptable error. In any event, the constraint set in the PSF domain is all of the complex functions that are identically equal to zero in any pixel outside the predefined narrow existence region. The projection onto the constraint set in the PSF domain is performed by multiplying the PSF by a function that is equal to 1 inside the narrow existence region of the PSF, and equals 0 elsewhere. In the case of the 1D DIPCH, the random-constrained PSF is limited to a narrow strip of columns, whereas in the case of the 2D DIPCH this PSF is limited to a narrow ring. In the end of the process, the POCS algorithm yields the suitable random-constrained PSF that is used in the hologram generation process. Figs. 6(b) and 6(c) show the phase distributions of the resulting PSFs of the 1D and the 2D DIPCHs, respectively, after applying the POCS algorithm for each of these cases.

Let us compare the reconstruction resolutions of the DIMFH and the DIPCH. Far objects captured by the DIMFH are reconstructed with a reduced resolution because of two reasons: (a) Due to the parallax effect, farther objects 'move' slower throughout the projections, and therefore they sample a magnified version of the generating PSF. This magnified version has narrower bandwidth, and thus the reconstruction resolution of farther objects decreases; (b) The quadratic phase function used in the DIMFH has lower frequencies as one approaches its origin. Since far objects are correlated with the central part of the quadratic phase function along a range that becomes shorter as the object is farther, the bandwidth of the DIMFH of far objects becomes even narrower beyond the bandwidth reduction mentioned in (a). In contrast to the DIMFH, the spatial frequencies of the DIPCH's PSF are distributed uniformly all over its area. Therefore, the DIPCH sustain resolution reduction of far objects only due to reason (a). Hence, the images of far objects reconstructed from the DIPCH, besides being protected by the random-constrained PSF, also have higher resolution.
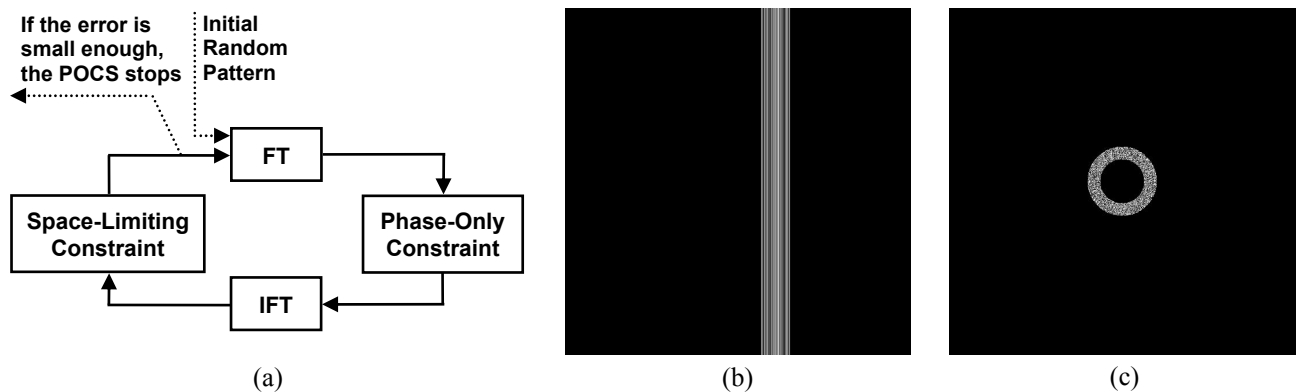

(a) (b) (c)

Fig. 6. (a) Schematics of the POCS algorithm for finding the PSF of the DIPCH; (b) The phase distribution of the generating random-constrained PSF of the 1D DIPCH; (c) Same as Fig. 6(b), but for the 2D DIPCH.

Now we show quantitatively that the resolution of far objects reconstructed from the DIMFH is worse than that of the DIPCH. The bandwidth of the generating PSF is determined by the 'movement' of the object point which is the closest to the imaging lens. For a distance of α between any two consecutive projections and for a distance of z_{min} between the closest object point and the imaging lens, the smallest shift that can be recorded on the camera is $\alpha f/z_{min}$, where f/z_{min} is the maximal magnification of the imaging lens. $\alpha f/z_{min}$ is also the minimal practical feature size of the generating PSF, because a smaller feature size cannot be detected by the camera due the minimal sampling gap of $\alpha f/z_{min}$. Therefore, the smallest object detail that can be recorded and reconstructed by the DIPCH is $\alpha f/(Mz_{min})$. Recalling that $M=f/z_s$, we realize that the DIPCH's resolution is linearly reduced for the far objects in the 3D scene.

For a single object point, the resulting hologram in the case of the DIMFH is exactly the PSF given by Eq. (14) or (15). These expressions are actually equal to the transfer function of a lens for which the resolution properties are well known. For a single point located at distance z_{min} from the imaging system, the width of the recorded hologram is $2K\alpha f/z_{min}$, and the smallest resolved detail is $\alpha f/(Mz_{min})$. Now, for a point located at distance z_s from the imaging system, the width of the recorded hologram is $2K\alpha f/z_s$. Since, as explained above, the DIMFH of an object point located at distance z_s from the imaging system is equivalent to a lens, the hologram resolving power is linearly dependent on its width. Thus, the resolved detail of an object at distance z_s is the smallest-ever resolved detail $\alpha f/(Mz_{min})$ multiplied by the ratio of the maximum hologram width, $2K\alpha f/z_{min}$, and the actual hologram width, $2K\alpha f/z_s$. Hence, the resolved detail of an object at a certain distance z_s is $\alpha f z_s/(Mz^2_{min})$ in the case of DIMFH. We recall that the size of the resolved detail in the case of the DIPCH is $\alpha f/(Mz_{min})$. Therefore, the ratio of the minimum resolved detail of the DIMFH and the DIPCH is z_s/z_{min}. This means that the farther the object from the imaging lens is, the worse the resolving power of the DIMFH, compared to the DIPCH, becomes. This conclusion is demonstrated in the results given next.

In Ref. [9], we have used the MVPs (the same MVPs which are used for the 1D DIMFH, and part of which is shown in Fig. 3) to generate a 1D DIPCH. The digital process of the DIPCH includes multiplying each of the acquired projections by the random-constrained PSF computed by the POCS algorithm and shown in Fig. 6(b). Each inner product is summed up into a single column in the 1D DIPCH, the amplitude and phase of which are shown in Figs. 7. To reconstruct this hologram, the DIPCH is convolved with the conjugate of a scaled version of the same PSF used for the hologram generation. The phases of the three reconstructing PSFs yielding the best in-focus reconstructed planes are shown in Figs. 8(a). The corresponding reconstructed planes are shown in Figs. 8(b). As before, in each of these planes, a different USAF chart is in focus, whereas the other two charts are out of focus. Once again, a resamapling process has to be applied along the horizontal axis of the reconstructed planes in order to retain the original aspect ratios of the objects. Figures 8(c) show these resampled best in-focus reconstructed planes, whereas Figs. 8(d) show the corresponding zoomed-in images of the in-focus charts in these three planes. Comparing Figs. 8(d) and 5(d), we conclude that farther objects have a higher resolution in the DIPCH than in the DIMFH. This property signifies the advantage of the DIPCH over the DIMFH, while the other advantage of the DIPCH being that it is protected by the random-constrained PSF used for generating and reconstructing the hologram.
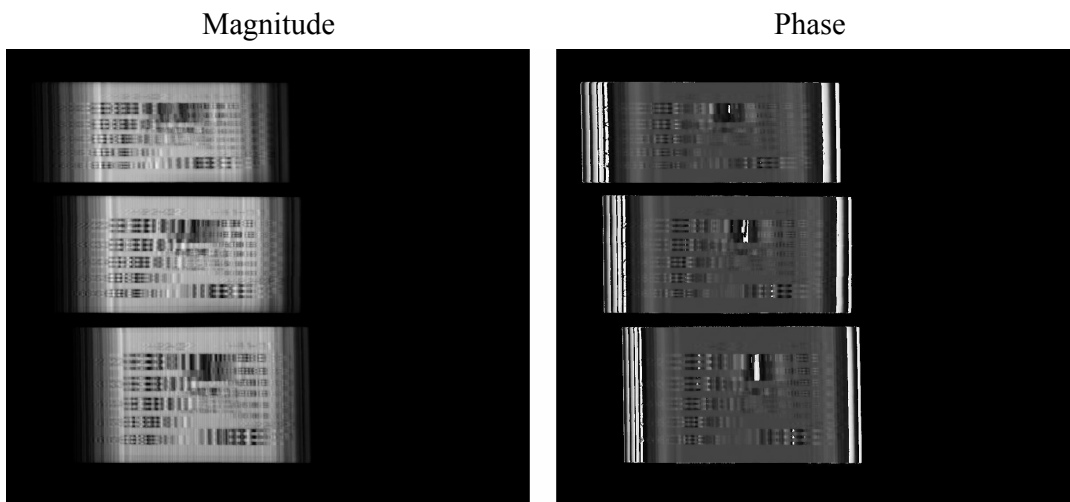
Magnitude　　　　　　　　　　　　　　　　Phase

Fig. 7. Magnitude and phase of the 1D DIPCH obtained from the MVP set, partially shown in Figs. 3(b).
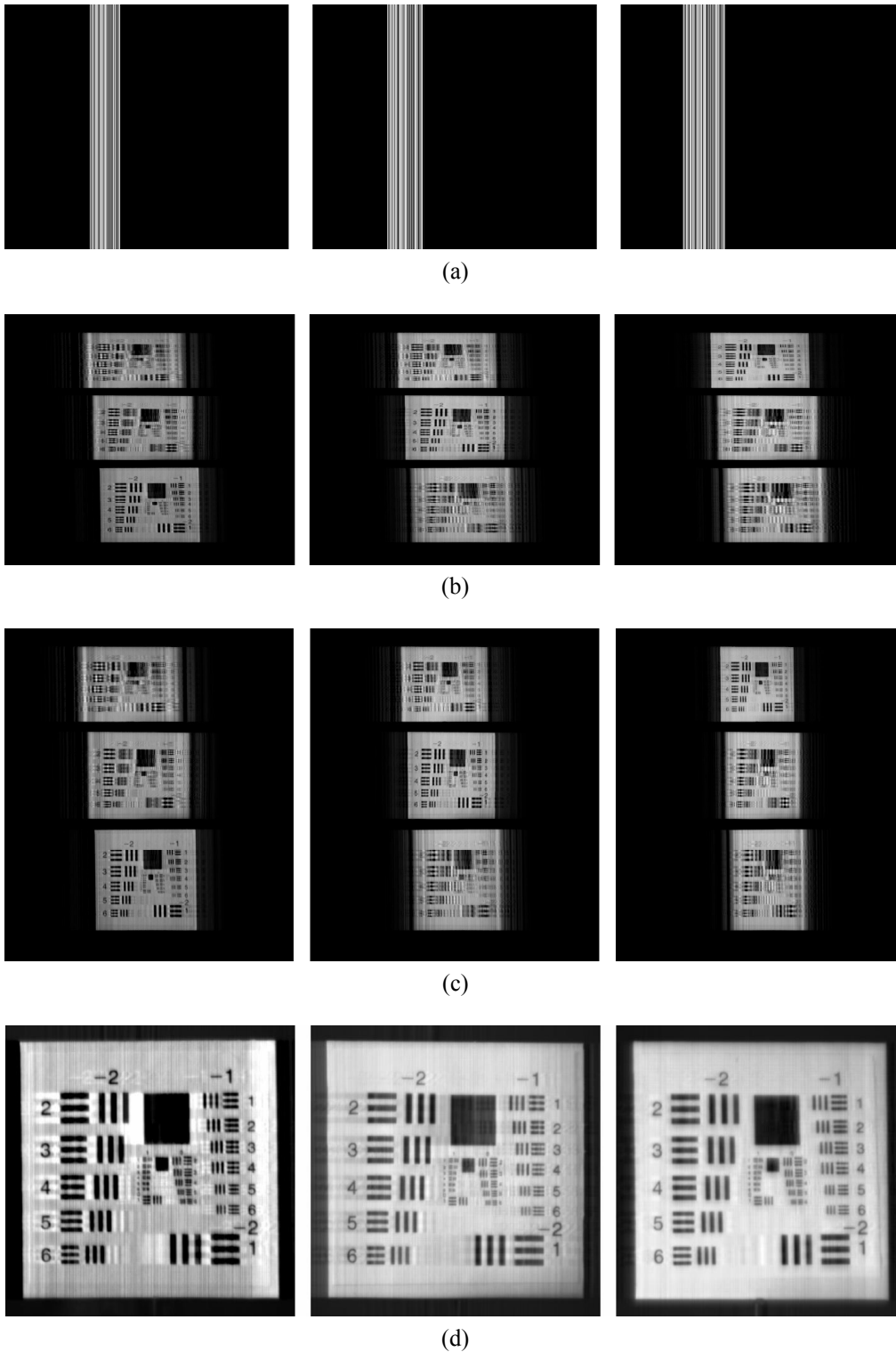
Fig. 8. Reconstructing the 1D DIPCH shown in Figs. 7: (a) The phase distribution of the reconstructing PSFs used for obtaining the three best in-focus reconstructed planes; (b) The corresponding three best in-focus reconstructed planes along the optical axis; (c) Same as Figs. 8(b), but after the resampling along the horizontal axis; (d) Zoomed-in images of the corresponding best in-focus reconstructed objects.

4. CONCLUSIONS

We have reviewed several methods for generating different types of MVP holograms. The MVPs of the 3D scene are captured by a simple digital camera, working under incoherent white light illumination, and then processed into a digital hologram of the scene. We have presented several different methods for capturing the MVPs, such as mechanical movement of the camera, using microlens, macrolens, or camera arrays, as well as applying the view synthesis algorithm for interpolating middle MVPs. The digital process applied to the acquired projections determines the type of hologram generated. It has been shown that it is possible to generate both 1D and 2D MVP holograms, and for each of them it is possible to generate regular types of holograms such as Fourier holograms and Fresnel holograms, as well as new types of correlation holograms such as the DIMFH and the DIPCH. The two latter holograms have advantages over the regular types of holograms since they are generated by straightforwardly processing the MVPs without redundant calculations, approximations, or assumptions. In addition, the DIPCH is scrambled by its PSF, so that only an authorized user can reconstruct the 3D scene, and besides, it has a higher resolution than the DIMFH due to a smart choice of its generating PSF. A unique feature of the DIMFH and the DIPCH is the fact that their transversal magnifications are constant and independent from the axial distance between the object and the camera. This effect can be eliminated during the reconstruction process. However, this feature can be utilized for optical pattern recognition, since a single matched filter can be used to detect all originally-equal objects in the scene without dependency on their axial distance from the camera. The prospective goal of the presented holographic methods is to facilitate the design of a simple and portable holographic camera that can be beneficial for a variety of practical applications, which include microscopy, 3D medical imaging, and 3D video acquisition for entertainment purposes.

REFERENCES

[1] Yatagai, T., "Stereoscopic approach to 3-D display using computer-generated holograms," Appl. Opt. 15, 2722-2729 (1976).

[2] Li, Y., Abookasis, D. and Rosen, J., "Computer-generated holograms of three-dimensional realistic objects recorded without wave interference," Appl. Opt. 40, 2864-2870 (2001).

[3] Abookasis, D. and Rosen, J., "Computer-generated holograms of three-dimensional objects synthesized from their multiple angular viewpoints," J. Opt. Soc. Am. A 20, 1537-1545 (2003).

[4] Sando, Y., Itoh, M. and Yatagai, T., "Holographic three-dimensional display synthesized from three-dimensional Fourier spectra of real existing objects," Opt. Lett. 28, 2518-2520 (2003).

[5] Abookasis, D. and Rosen, J., "Three types of computer-generated hologram synthesized from multiple angular viewpoints of a three-dimensional scene," Appl. Opt. 45, 6533-6538 (2006).

[6] Shaked, N. T., Rosen, J. and Stern, A., "Integral holography: white-light single-shot hologram acquisition," Opt. Express 15, 5754-5760 (2007).

[7] Katz, B., Shaked, N. T. and Rosen, J., "Synthesizing computer generated holograms with reduced number of perspective projections," Opt. Express 15, 13250-13255 (2007).

[8] Shaked, N. T. and Rosen, J., "Modified Fresnel computer generated hologram directly recorded by multiple viewpoint projections," Accepted for Publication to Appl. Opt. – Special Issue on Digital Holography (To be published in July 2008).

[9] Shaked, N. T. and Rosen, J., "Multiple viewpoint projection holograms synthesized by spatially-incoherent correlation with a general function," Submitted for publication to J. Opt. Soc. Am. A.

[10] Stern, A. and Javidi, B., "Three dimensional sensing, visualization, and processing using integral imaging," Procs. of IEEE 94, 591 (2006).

[11] Scharstein, D., [View Synthesis Using Stereo Vision], Lecture Notes in Computer Science (LNCS) 1583, Springer-Verlag, Berlin, Chap. 2 (1999).

[12] Abookasis, D. and Rosen, J., "Digital correlation holograms implemented on a joint transform correlator," Opt. Commun. 225, 31-37 (2003).

[13] Javidi, B. and Sergent, A., "Fully phase encoded key and biometrics for security verification," Opt. Eng. 36, 935-942 (1997).

[14] Fienup, J. R., "Phase retrieval algorithm: a comparison," Appl. Opt. 21, 2758-2769 (1982).

[15] Stark, H. (Ed.), [Image Recovery: Theory and Application], Academic Press, Orlando, 29-78 & 277-320 (1987).